Supporting information

For

Reversible engineering of spin-orbit coupling in monolayer MoS_2 via laser irradiation under controlled gas atmospheres

Xilong Liang,[1,2] Chengbing Qin,[1,2*] Yan Gao,[1,2,3] Shuangping Han,[1,2] Guofeng Zhang,[1,2] Ruiyun Chen,[1,2] Jianyong Hu,[1,2] Liantuan Xiao,[1,2*] and Suotang Jia[1,2]

[1] State Key Laboratory of Quantum Optics and Quantum Optics Devices, Institute of Laser Spectroscopy, Shanxi University, Taiyuan, Shanxi 030006, China.

[2] Collaborative Innovation Center of Extreme Optics, Shanxi University, Taiyuan, Shanxi 030006, China.

[3] Department of Physics, Shanxi Datong University, Datong, 037009, China.

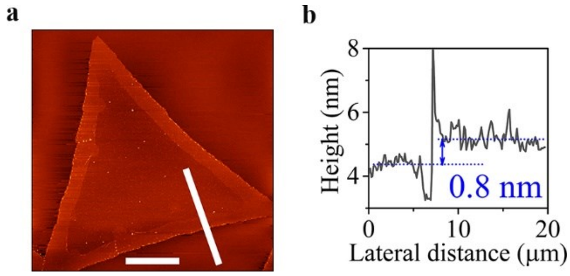

Figure S1. (a) AFM image of the prepared sample. (b) Height profiles corresponding to the solid line in a. The thickness of ~0.8 nm confirms that the prepared sample is monolayer.

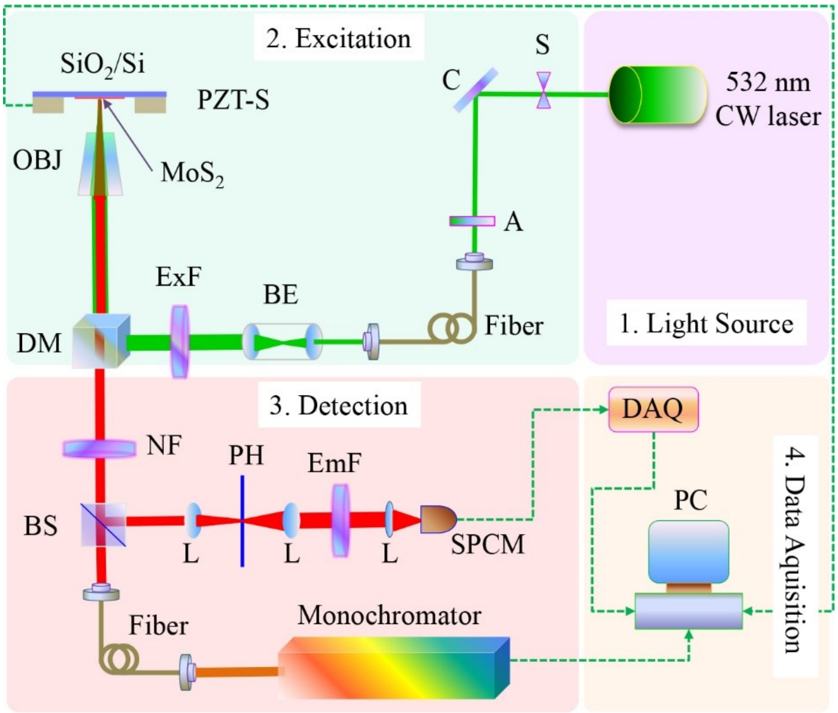

Figure S2. Schematic diagram of the optical setup. S: shutter; C: beam combiner; A: attenuator; BE: beam expander; ExF: excitation filter; DM: dichroic mirror; OBJ: objective; PZT-S: piezo-electric translation nano-stage; NF: notch filter; BS: beam splitter; L: lens; PH: pinhole; EmF: emission filter; SPCM: single-photon counting modular; DAQ: data acquisition card; PC: personal computer.

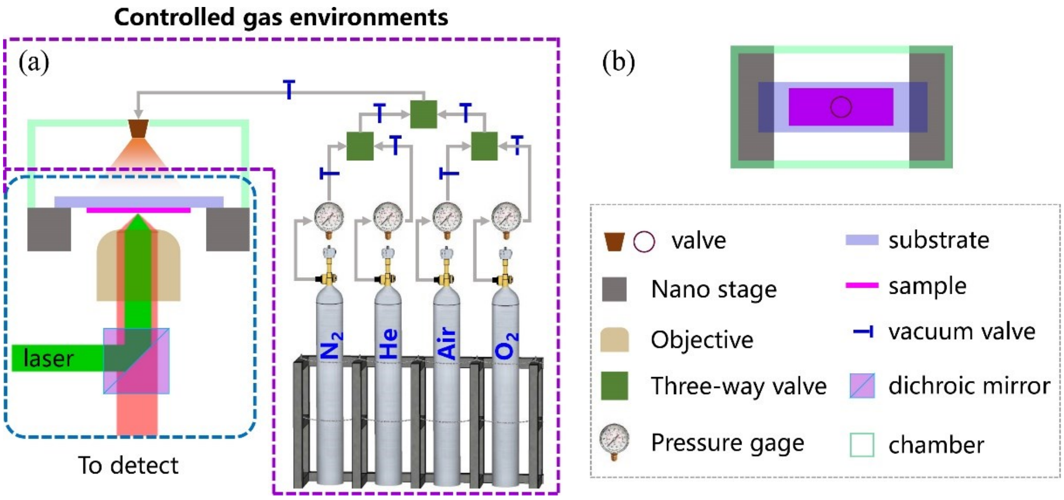

Figure S3. Schematic illustration of the controlled gas environments. (a) Gases were blowing from the backside of the substrate; the bottom of the chamber was opened. The blowing rate of gases was kept constant at 1 L/min. PL quenching processes were performed by just stopping to blow N_2, rather than sweeping the dry air gases. (b) Top view of the setup.

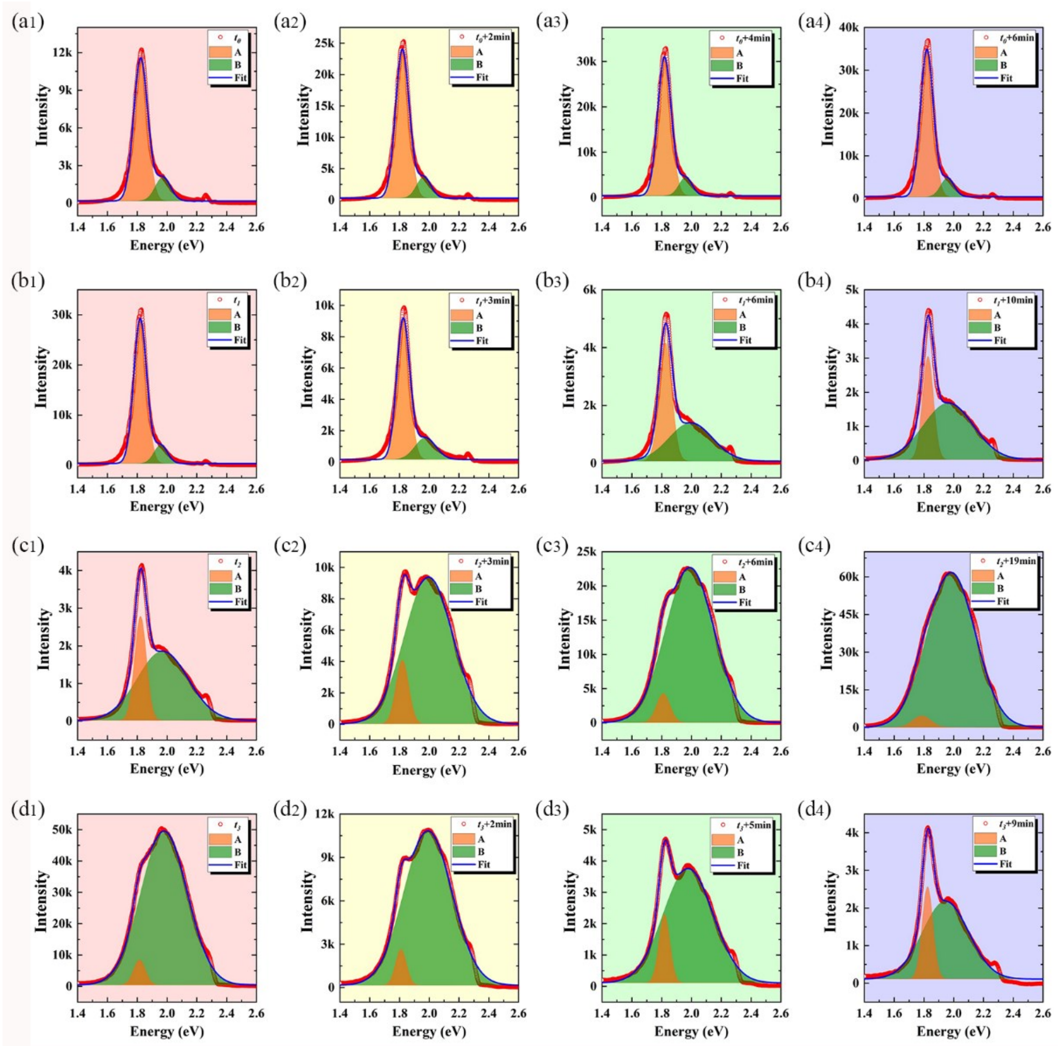

Figure S4. Typical fitting results for the spectral profiles for the four stages presented in Figure 3a. The orange area denotes A exciton, and the green area denotes B exciton. (a) Stage I, with the prolonged irradiation times, slight increase in B exciton can be observed. (b) Stage II, with the increase of irradiation times, the full PL intensity reduce. The ratio of B exciton strongly increases and broaden. (c) Stage III, the ratios of B exciton are dramatically enhanced, the ratios of A exciton reduce sharply. (d) Stage IV, the ratios of A and B excitons gradually recovered to (c1).

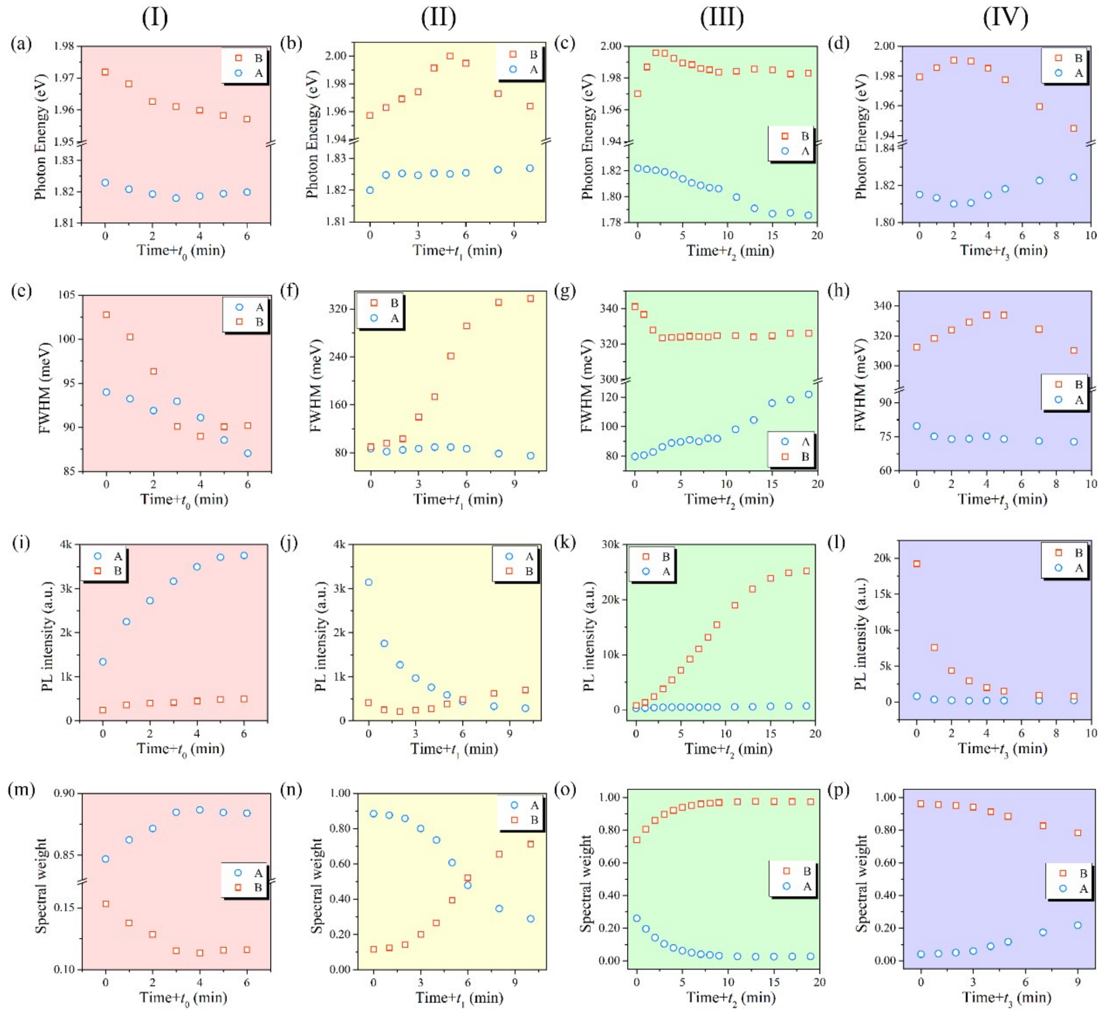

Figure S5. Comparison of the determined parameters during different stages. (a-d) Photon energies, (e-h) FWHM, (i-l) PL intensities, and (m-p) spectral weights of A and B excitons as a function of irradiation times. Variations and comparisons of each parameter during different stages can be clearly determined.

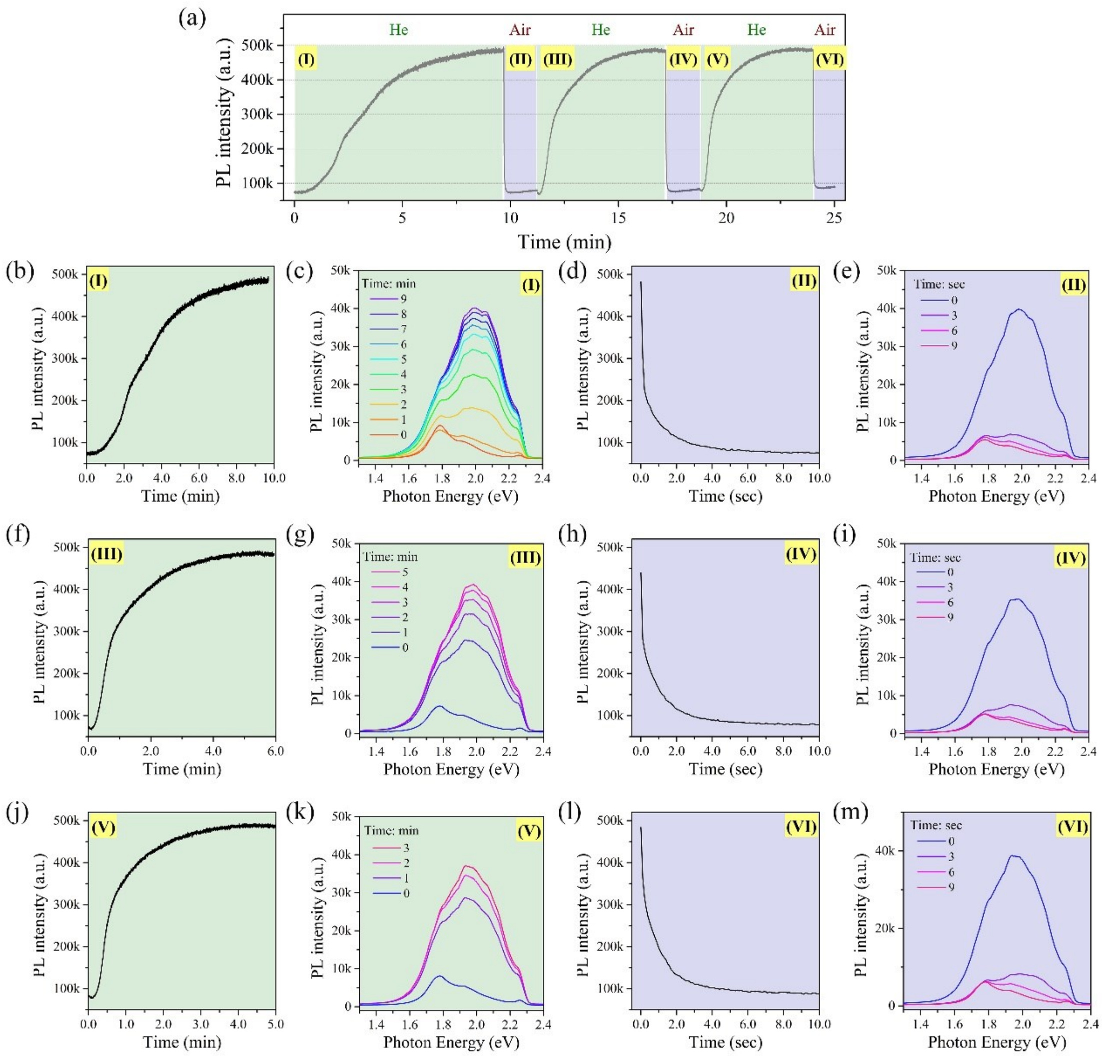

Figure S6. PL behavior and spectra evolution of monolayer MoS_2 against gas cycling between helium (He) and air atmosphere. In the He atmosphere, PL gradually enhanced and tended to stabilize in several minutes. In contrast, PL sharply quenched in several seconds when we stopped blowing He. The corresponding spectral profiles can be recovered as well. These phenomena were the same as those performed in N_2 and air conditions.

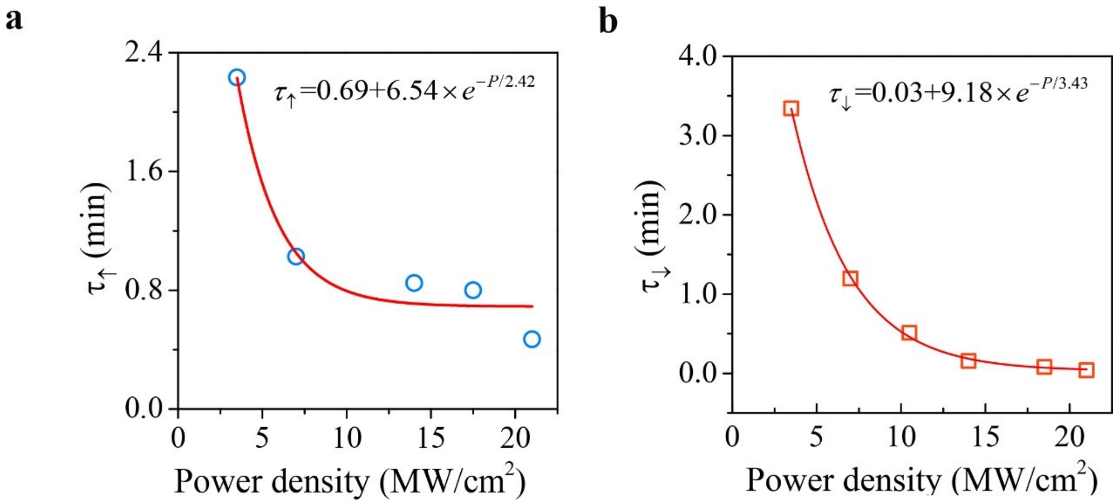

Figure S7. The fitting enhancement rate $\tau_\uparrow$ (a) and quenching rate $\tau_\downarrow$ (b) as a function of excitation power density. The solid lines are the fitting results, the corresponding parameters have been labeled in figures.

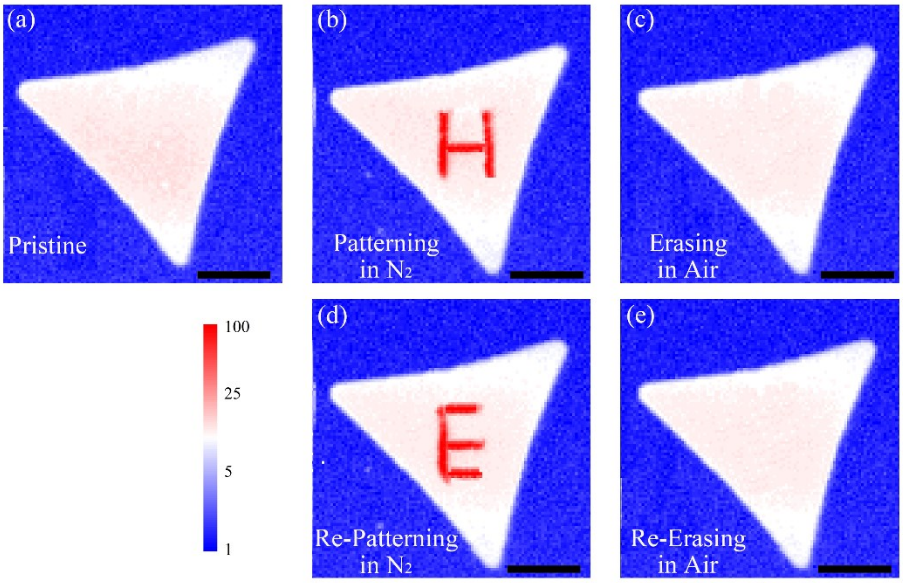

Figure S8. Erasable patterning of microstructures on monolayer MoS_2 by laser irradiation via gas cycling. (a) PL image of the pristine sample. (b) Pattering an alphabet ("H") on monolayer MoS_2 by 532 nm irradiation in N_2 atmosphere. (c) Erasing the patterning by re-irradiation in air condition. (d, e) are the repetitive operation as that in (b, c) but another alphabet ("E"). The power of irradiation laser was 21 MW/cm^2, the power of the reading laser was 5 kW/cm^2. Scale bar: 10 μm.